Journal of Cell Science 112, 877-886 (1999)
Printed in Great Britain © The Company of Biologists Limited 1999
JCS9903

Myosin II-independent F-actin flow contributes to cell locomotion in *Dictyostelium*

Yoshio Fukui[1,*], Toshiko Kitanishi-Yumura[2] and Shigehiko Yumura[2]

[1]Cell and Molecular Biology, Northwestern University Medical School, Chicago, Illinois
[2]Department of Biology, Faculty of Science, Yamaguchi University, Yamaguchi, Japan
*Author for correspondence (e-mail: y-fukui@nwu.edu; web site: http://pubweb.nwu.edu/~yoshifk/fukui.html)

Accepted 4 January; published on WWW 25 February 1999

SUMMARY

While the treadmilling and retrograde flow of F-actin are believed to be responsible for the protrusion of leading edges, little is known about the mechanism that brings the posterior cell body forward. To elucidate the mechanism for global cell locomotion, we examined the organizational changes of filamentous (F-) actin in live *Dictyostelium discoideum*. We labeled F-actin with a trace amount of fluorescent phalloidin and analyzed its dynamics in nearly two-dimensional cells by using a sensitive, high-resolution charge-coupled device. We optically resolved a cyclic mode of tightening and loosening of fibrous cortical F-actin and quantitated its flow by measuring temporal and spatial intensity changes. The rate of F-actin flow was evaluated with respect to migration velocity and morphometric changes. In migrating monopodial cells, the cortical F-actin encircling the posterior cell body gradually accumulated into the tail end at a speed of 0.35 μm/minute. We show qualitatively and quantitatively that the F-actin flow is closely associated with cell migration. Similarly, in dividing cells, the cortical F-actin accumulated into the cleavage furrow. Although five times slower than the wild type, the F-actin also flows rearward in migrating *mhcA*$^{-}$ cells demonstrating that myosin II ('conventional' myosin) is not absolutely required for the observed dynamics of F-actin. Yet consistent with the reported transportation of ConA-beads, the direction of observed F-actin flow in *Dictyostelium* is conceptually opposite from a barbed-end binding to the plasma membrane. This study suggests that the posterior end of the cell has a unique motif that tugs the cortical actin layer rearward by means of a mechanism independent from myosin II; this mechanism may be also involved in cleavage furrow formation.

Key words: Amoeboid movement, Cytokinesis, *Dictyostelium*, F-actin, Locomotion

INTRODUCTION

Dictyostelium represents a group of highly motile amoeboid cells that share many common features with mammalian cells (Harris, 1994). In fact, the 'inch worm model' for fibroblast locomotion (Alberts et al., 1994) and the 'three-step model' for amoeboid locomotion (Fukui and Yumura, 1986) both depict three common processes, i.e. protrusion, retraction, and contraction. However, the architectural dynamics of actin and its relevance to locomotion in *Dictyostelium* cells have not been elucidated. The reason is technical, since cells are small and locomotion and shape changes are rapid.

Past immunofluorescence and ultrastructural studies have revealed the presence of distinctive organizations of F-actin in *Dictyostelium*: three-dimensional meshworks in pseudopodia (Condeelis, 1993; Cox et al., 1995), cortical bundles or meshworks with increased thickness towards the rear (Yumura et al., 1984; Fukui and Yumura, 1986; Fukui, 1993), and radial arrays emerging from postulated adhesion sites (Yumura and Kitanishi-Yumura, 1990; Fukui and Inoué, 1997). Neither the precise organization nor the function of these F-actin structures has been elucidated. Therefore, it is important to study the in vivo organization of different F-actin structures with respect to binding proteins and specific roles in cell locomotion.

The rearward traction forces are believed to be translated into the retrograde transport of surface markers (Harris, 1994). This particle transport has been studied in detail in fibroblasts (Abercrombie et al., 1970; Harris, 1973; Jacobson, et al., 1984), nerve axons (Bray, 1970; Forscher and Smith, 1988), leukocytes (Harris, 1973; Lee et al., 1990), macrophages (Dembo and Harris, 1981; Sheetz et al., 1989), fish keratocytes (Lee et al., 1993), and *Amoeba* (Grebecki, 1994). It is widely believed that the traction forces for the particle transport are driven by the cytoskeleton through crosslinks via membrane glycoproteins (Jacobson et al., 1984; Sheetz et al., 1989; Holifield et al., 1990). In *Dictyostelium*, the particle transport was first described by Shaffer (1962) and, more recently, Jay and Elson (1992) performed a detailed analysis. They found that ConA-coated particles move from the leading edge all the way to the tail of locomoting amoebae and this transport also occurs in myosin II knock out cells.

In general, the actin-based and myosin-based mechanisms

are believed to contribute to the surface particle movement and likewise to cell locomotion (Harris, 1994). The 'treadmilling' of actin (Wang, 1985) represents the actin-based mechanism (Heath and Holifield, 1991b). This theory proposes the forces driven by the predominant elongation of F-actin at the fast-growing, barbed end (Pollard and Craig, 1982), which has been also demonstrated in vivo to be the preferred site for binding to the plasma membrane (Small et al., 1978; Small, 1981; Tilney and Inoué, 1985; Svitkina et al., 1986; Carlier, 1998). In neuronal growth cones, the involvement of myosin in retrograde flow of F-actin and growth of filopodia has been suggested (Lin et al., 1996). Importantly, however, these mechanisms have been examined only with respect to the protrusion of the anterior structures (lamellipodia and filopodia) but the mechanism that brings the posterior cell body (behind lamellipodia) forward has not been attested.

The paradigm of actin mechanistics is that G-actin must be added primarily to the barbed end at the frontal membrane and transported towards the rear, generally up to the region containing the nucleus. The studies by Theriot and Mitchison (1991) and Symons and Mitchison (1991), however, demonstrated the organization and dynamics of F-actin in fish keratocytes ('nucleation-release' model) and fibroblasts ('gradient of filament length') that are contradictory to the long-believed treadmilling/cortical flow mechanism. Whether the above conflicting results came from different techniques (fluorescence recovery after photobleaching vs photoactivation), or rather revealed different mechanisms has not been determined (Heath and Holifield, 1991a). With this respect, a recent study by Cramer et al. (1997), identifying the graded polarity of F-actin in locomoting fibroblasts, is inspiring. To date, however, it has not been determined what brings the *posterior* cell body forward and whether F-actin flow occurs in the rear cell cortex. Should the flow occur, how is F-actin organized and how can flow be translated into the traction forces in the rear cell body? It is also important to determine *if* myosins are involved, and how they might contribute to these movements.

In the present study, we determined gentle conditions for loading fl-phalloidin and, using this method, monitored very low level fluorescence with high spatial resolution. We demonstrate that the cortical F-actin layer encompassing the posterior cell body flows all the way to the tail as the cell migrates; this flow does not absolutely require myosin II. The observed flow is conceptually paradoxical to the generally believed F-actin orientation, i.e. barbed-end binding with the plasma membrane (reviewed by Small, 1994). We suggest possible models for the cortical F-actin flow and its role in amoeboid locomotion and cytokinesis.

MATERIALS AND METHODS

Cells and culture

Dictyostelium discoideum (strain NC4) cells were cultured with *Escherichia coli* (strain B/r) on nutrient agar plates (Fukui and Inoué, 1991). Myosin heavy chains-null cells (*mhcA*$^{-}$; Manstein et al., 1989) were cultured in 9 cm-diameter plastic dishes with HL5 medium. Cells were scraped with silicone rubber and washed with cold 15 mM Na/K phosphate buffer (pH 6.4). They were spread on non-nutrient agar plates and incubated for 3-4 hours at 22°C before electroporation.

Electroporation

Fluorescently labeled phalloidin was loaded into cells by electroporation using the method modified from Yumura (1996). The cells were centrifuged at 300 ***g*** for 1.5 minutes and suspended in phosphate buffer to make a 10^8 cells/ml suspension. FITC-phalloidin (100 μg) was dissolved in a mixture of 80 μl of methanol and 25 μl of dimethylsulfoxide. After placing in a ventilated sterile hood for several hours to evaporate off the methanol, the solution was diluted with 100 μl of the phosphate buffer. An equal volume (20 μl) of cell suspension and FITC-phalloidin (80 μM in 20% dimethylsulfoxide) (P-5282: Sigma Co., St Louis, MO) were mixed in a pre-cooled electroporation cuvette (1 mm of interelectrode space; #165-0289: Bio-Rad Laboratories, Richmond, CA). The unit was discharged at 3 μF at 220 V using a Bio-Rad Gene Pulser II. The cells were immediately washed with cold phosphate buffer.

Fluorescence microscopy and digital image acquisition

After electroporation, the cells were allowed to settle on a 22 × 22 mm glass coverslip (no. 1-1/2: Corning Glass Works, Corning, NY) and overlaid with a 0.15 mm-thick, 2% agarose sheet (agarose-M: Pharmacia LKB, Uppsala, Sweden) (Fukui and Inoué, 1991). The coverslip was inverted and placed on a glass slide topped with spacers made of 0.15 mm-thick two-sided adhesive tape. The sample was sealed with a 1:1:1 mixture of lanolin, vaseline, and bee's wax (LAVAB) (Fukui and Inoué, 1997). The sample was observed under an epifluorescence microscope (Axioskop-50: Carl Zeiss, Inc., Thornwood, NY) equipped with an oil-immersion ×63 plan apo objective (NA 1.4). The image was acquired with a cooled CCD (PXL: Photometrics Ltd, Tucson, AZ) installed with a Kodak KAF 1400 chip. The fluorescence and phase-contrast images were sequentially acquired at 8-bits of depth of gray scale using a filter wheel (Lambda10-2: Sutter Instrument Co., Novato, CA) and an electric shutter (UniBlitz D122: Vincent Associate, Rochester, NY). The acquisition time was 50-300 milliseconds and the interval between different paths was about 5 milliseconds; they were controlled by the parallel port controller. The image acquisition was automated by customized journals installed into an integrated image acquisition and processing system (MetaMorph: Universal Imaging Corporation, West Chester, PA). The spatial resolution of our system has been estimated to be 250 nm (Yumura and Fukui, 1998).

Transmission electron microscopy

Small droplets of cell suspension were placed on carbon-coated plastic coverslips. After the cells started migrating (ca. 2 hours), the samples were processed for the agar-overlay method described in the section above. The samples were fixed with a mixture of 1% formaldehyde (Polysciences, Inc., Warrington, PA; cat. #18814) and 0.4% glutaraldehyde (Polysciences, Inc.; cat. #00216) in MFSS buffer (50 mM Hepes, pH 7.5, 5 mM EDTA, 5 mM EGTA, 50 mM KCl) for 5 minutes at room temperature. For preparation of the cytoskeleton, the cells under the agarose were permeabilized with a mixture of 0.5% Triton X-100 and 0.5% digitonin (Sigma Chemicals, St Louise, MO; cat. D-1407) for 10 minutes at room temperature in the presence of 1% formaldehyde, 0.4% glutaraldehyde, 0.1% 3-maleimidobenzoic acid *N*-hydrosuccinimido ester (Sigma Chemicals; M-2786), and 0.2% tannic acid (Tousimis Research Corp., Hockville, MD; cat. #4241) in MFSS buffer. The samples were post-fixed with 1% OsO_4 in 15 mM Na/K-phosphate buffer (pH 6.4) for 30 minutes. After dehydration through an ethanol series, the samples were embedded with Spurr's low-viscosity medium (Polysciences, Inc.; cat. #01916). The coverslips were then removed and the samples were re-embedded with Spurr's medium. After staining with uranyl acetate and lead citrate, thin sections were observed under a transmission electron microscope (JEOL, Peabody, MA; model JEM-100CX).

RESULTS

Fl-phalloidin is bound to F-actin in the posterior cell cortex

After attaching onto the substratum, the cells loaded with fl-phalloidin resumed the migration in 20-30 minutes (the control cells loaded with the buffer started moving in 5-10 minutes). Under the fluorescence microscope, about 15% of the cells exhibited fluorescence. Highly fluorescent cells did not resume the migration after 30 minutes and were omitted from further observation. Weakly to moderately fluorescent cells did migrate and were examined for the following analyses. During the recovery period, both fl-phalloidin-loaded and control cells were spherical and non-motile. Towards the end of this period, fl-phalloidin was observed gradually accumulating into the cortical layer. The effects of fl-phalloidin in moderately fluorescent cells seem to be non-hazardous since the cells continued to migrate and divide normally. The fluorescence eventually disappeared after several hours.

The through-focus observation indicated that, in a cross-sectioned view, the cortical F-actin layer encircles the entire posterior cortex of the nearly two-dimensional cell. By TEM (Fig. 1), we show that the cortical F-actin is organized into an amorphous, fibrous submembranous meshwork surrounding the posterior cell body (Fig. 1B: white arrows), while, in the anterior pseudopodium, it is assembled into a massive 3-D network (Fig. 1B: dotted black square). Note that the posterior end has the thickest cortical layer (Fig. 1A: thin arrows). In this report, we define the 'cortical F-actin' as the F-actin layer underlying the plasma membrane wrapping the entire *'posterior'* cell body; i.e. *behind the pseudopodium* (Fig. 1C,D: darkly shaded area). Consistent with previous studies (Wehland and Weber, 1981; Wang, 1987), fl-phalloidin did not exhibit conspicuous fluorescence in the leading edge. Therefore, in this study, we only examined the F-actin dynamics in the posterior cell body. For the mechanism of pseudopodial protrusion, see Condeelis (1993).

To determine whether most fl-phalloidin was incorporated into F-actin or there was a considerable amount of free fl-phalloidin in the cytoplasm, we compared the rate of quenching of the fluorophore occurring in a 10×10 pixel area either in the cortex or the ground cytoplasm (Fig. 2). The result showed that the kinetics of the quenching are similar, for at least up to 70 seconds' total excitation. This result indicates that there is little, if any, free fl-phalloidin in the ground cytoplasm.

Architectural dynamics of cortical F-actin demonstrates its mobility

When the cells resumed motility, they actively projected pseudopodia, initially in a random fashion. Fig. 3 shows a representative sequence qualitatively illustrating this mode of F-actin dynamics. The actual sequence consists of 30 images recorded for a 10 minute period but only the early part is shown in the representative figure (the full sequence can be seen as a movie at our Web site). The result shows that the fl-phalloidin is predominantly bound to the cortical layer. When the cell transiently becomes polarized, fl-F-actin surrounds the posterior cell body (frames a-d). It should be noted that, in non-migrating cells, fl-F-actin does not accumulate into the posterior cortex. This is in marked contrast to migrating amoebae (Fig. 4: following section). Also note that fl-phalloidin does not incorporate into the pseudopodium (a large arrow marked 1). This result is consistent with the earlier observations that the fl-phalloidin does not assemble into F-actin in leading edges, but it is a reliable marker for studying the slowly exchanging actin structures (Wehland et al., 1980;

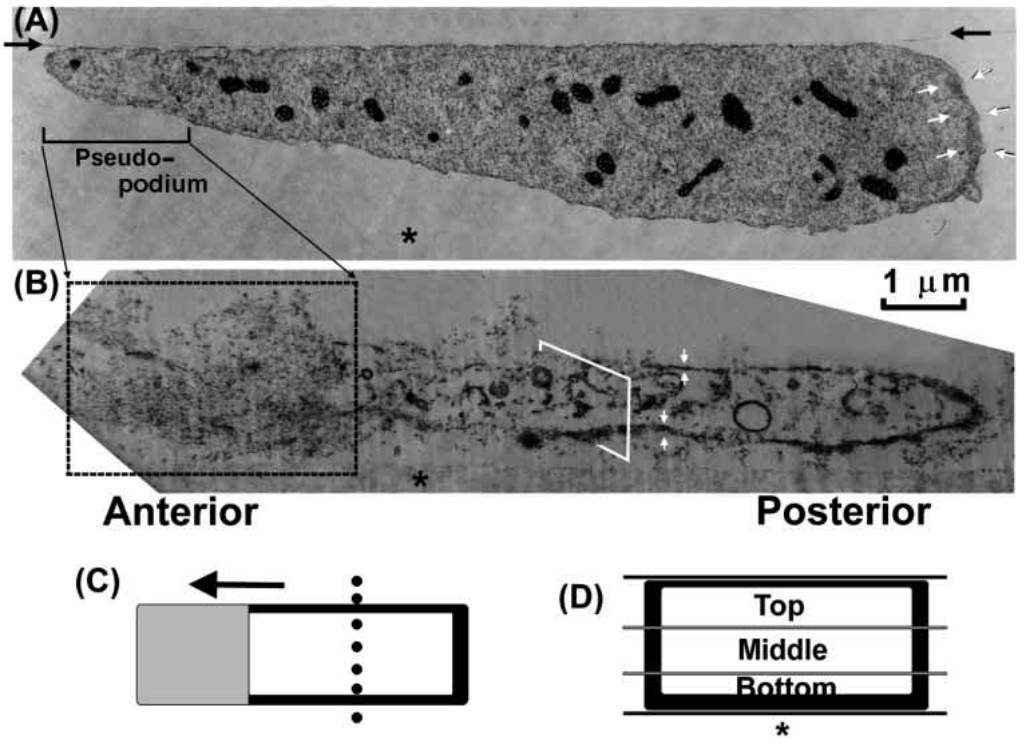

Fig. 1. Transmission electron micrographs of intact (A) and permeabilized (B) *Dictyostelium* amoebae showing the cortical F-actin layer. (A) Side view of an intact monopodial cell migrating towards the left. The electron opaque region in the anterior is the pseudopodium. The posterior cortex is surrounded by a thick F-actin layer (thin white arrows). (B) Side view of a permeabilized cell. F-actin in the pseudopodium shows an extensive meshwork (black box) while the entire posterior cell body is surrounded by a layer of F-actin. (C) A diagram illustrating the longitudinal overview of migrating amoeba. The cortical F-actin organizes into about 1 mm thick cortical layer in the posterior cell body. (D) An imaginary cross section view of the region marked with the dotted line in C. F-actin dynamics were examined in the posterior cortex *behind pseudopodium* corresponding to the area painted black. *, agarose.

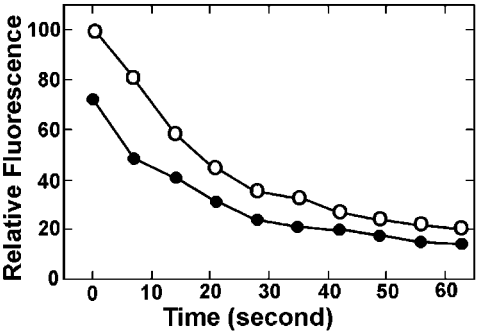

Fig. 2. The kinetics of fluorescence quenching of fl-phalloidin located in the cortex (open circles) or in the ground cytoplasm (closed circles) in live amoebae. The samples were continuously illuminated for a total of 70 seconds, and the intensity was measured every 7 seconds. The gray scale was measured as the total pixels accumulated in the 70 millisecond duration in a 10×10 pixel area, that was precisely positioned on either a cortical actin layer or the ground cytoplasm. The rate of quenching was very similar in both areas, indicating that most fl-phalloidin was incorporated into F-actin and that there was very little free fl-phalloidin diffusing in the ground cytoplasm.

Wehland and Weber, 1981; Wang, 1987; Cao and Wang, 1990; Lee et al., 1997).

The above results showed that F-actin labeled with fl-phalloidin is capable of integrating into functional actin-containing structures based on: (1) the dynamic positional and organizational changes of the cortical F-actin; (2) a tightening-loosening mode of architectural changes, particularly notable during the rounding up process (Fig. 3e,f: small arrows); and (3) changes in the number and orientation of the F-actin bundles seen in the overview (Fig. 3a-d: small arrows).

In Fig. 3h, we illustrate the mode of motility of this cell. The cell did not migrate but protruded and retracted several pseudopodia in different directions during the 10 minute observation period. The dynamics of the first major pseudopodium (labeled 1) are shown in a-g but the other three (labeled 2-4) that formed in the later sequence are not shown in this panel. The peak of the pseudopodia protrusion occurred at times 00:00 (1), 05:00 (2), 08:20 (3), and 10:00 (4) (data not shown). Note that the high intensity area is nearly circular, demonstrating that the fl-F-actin was mobile and continuously recruited into the position opposite from the protruding pseudopodium.

The intensity analysis demonstrates the retrograde flow of F-actin in migrating amoebae

In polarized cells, we found that fl-phalloidin is predominantly bound to F-actin surrounding the posterior cell body, and when the cell migrates, fl-F-actin moves towards the posterior end (Fig. 4). As in non-migrating cells, the cortical F-actin bundle exhibited a loosening and re-tightening mode of dynamics as demonstrated by the fluorescence sequence (arrows in a,c,e). During the few minutes of observation, the cortical F-actin gradually accumulated into the posterior end. (For complete phase-contrast and fluorescence sequences, see our Web site.)

Since the cells were nearly two-dimensional, the relative intensity is thought to represent the relative content of fl-phalloidin-F-actin in the cortical domain. In the following, the mode of rearward accumulation of F-actin was quantitatively analyzed by measuring the rate of intensity changes in selected

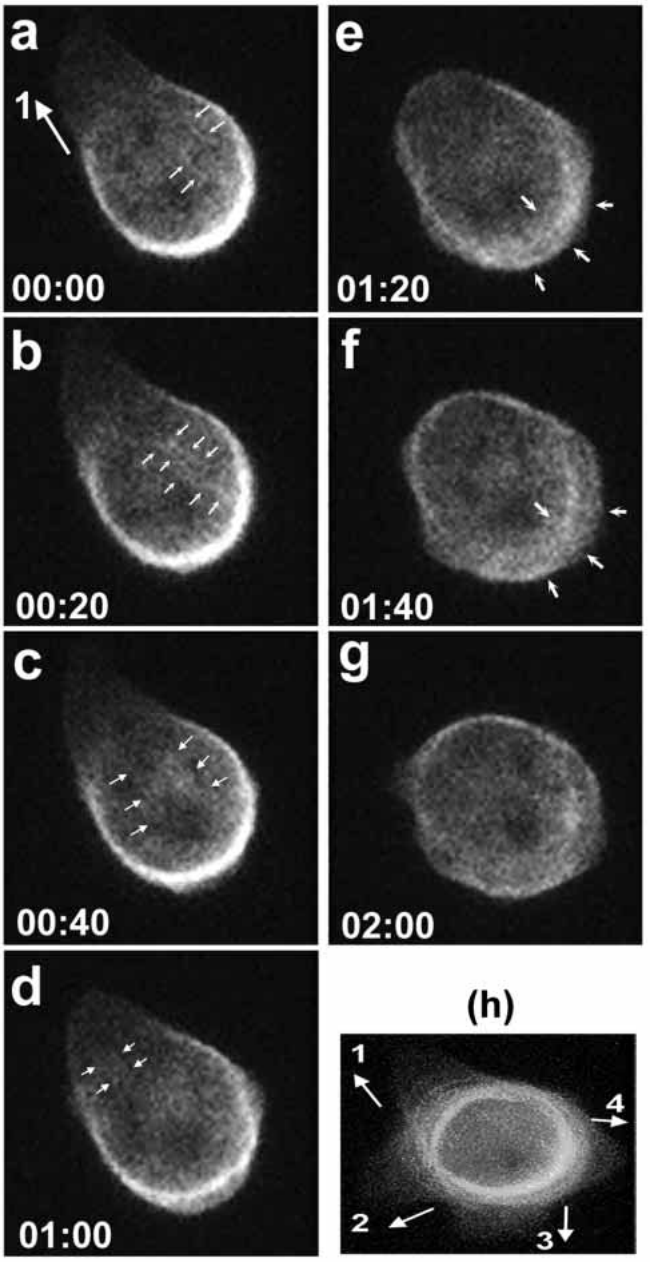

Fig. 3. Dynamic changes in the organization of fl-F-actin in non-migrating wild type *Dictyostelium* amoeba. Images were recorded every 20 seconds for 10 minutes (total 30 frames) but only the early 7 frames are shown. (a-g) A representative image sequence showing that the fl-F-actin is capable of re-organizing into various cortical regions reflecting the cell's behavioral changes. Note that the posterior F-actin bundle loosened (e,f: arrows), when the existing pseudopodium (a: large arrow marked 1) was replaced with a new pseudopodium (h: arrow marked 2). F-actin also exhibits a parallel array converging into the posterior body (a-d: small arrows). (h) An overlaid intensity profile illustrating the mode of motility during the entire period of observation. The numbered arrows indicate the pseudopodia formed in this order (only the first one is shown in a-g). The movie showing the whole sequence can be seen at our Web site. Time in min:sec.

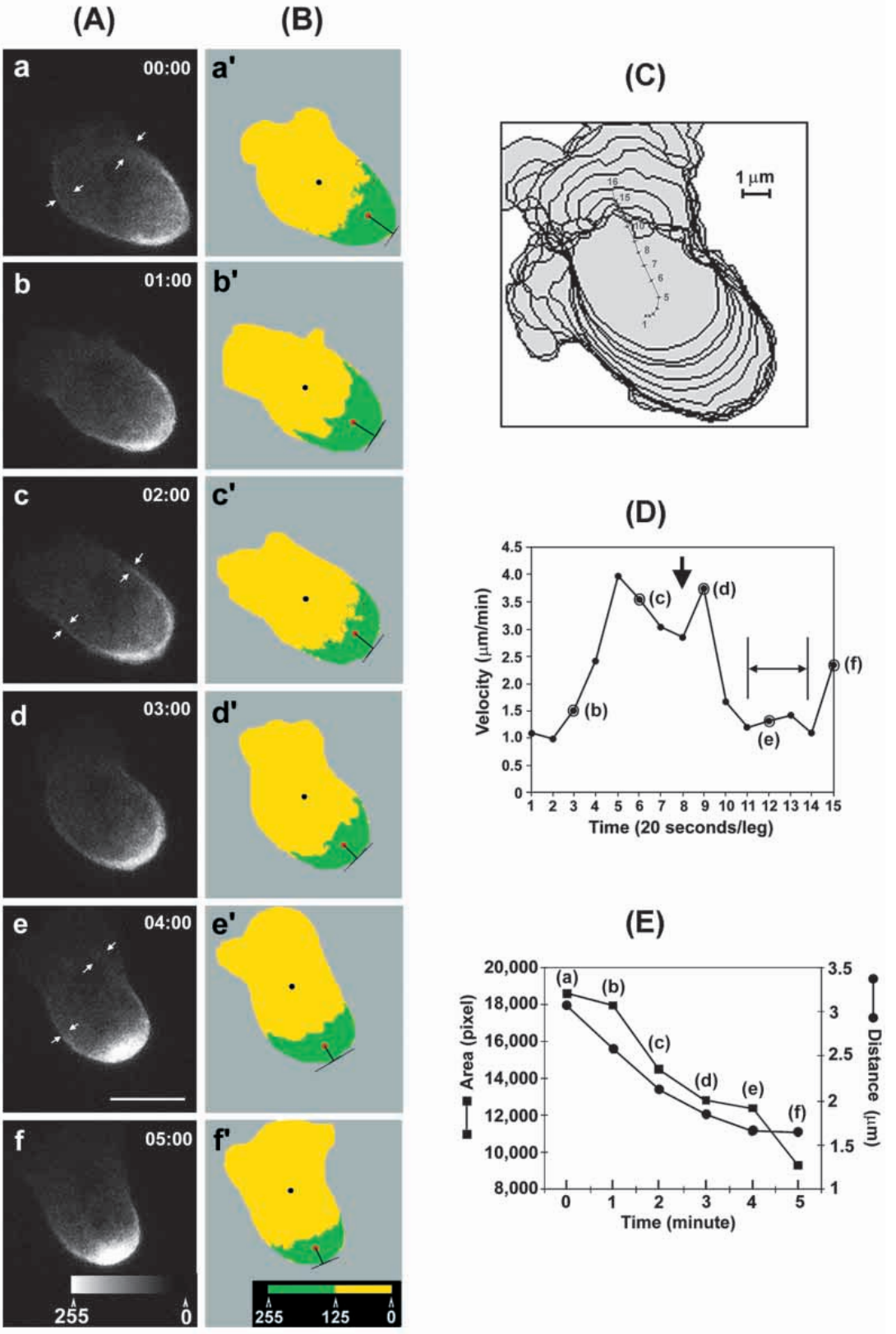

Fig. 4. Representative sequence showing the dynamics of fl-F-actin in migrating wild type amoebae. (A) Fluorescence images shown with 8-bit depth of intensity. The actual images were acquired every 20 seconds but this sequence only shows selected frames. Note that the cortical F-actin bundles exhibited a cycling tightening and loosening (small arrows in a, c, e). Time in min:sec. Bar, 5 μm. (B) A diagram illustrating the geometric relation of the high intensity area (green) relative to the cell periphery (yellow) and the centroid (black dot). Red dot = intensity center. (C) A diagram showing the cell periphery and the centroid position illustrating the overall migratory behavior. (D) Changes in the migration velocity as demonstrated by the centroid translocation (av., 2.14 μm/minute). The labels a-f indicate the corresponding frames in A. The velocity slightly dropped (arrow) when the cell changed the migration direction by projecting a new pseudopodium towards a new direction (d in A), while the velocity remained low (bracket) during the contact inhibition. (E) The retrograde flow of fl-F-actin as demonstrated by the condensation of high intensity area (square) and the movement of the intensity center (circle: av., 0.35 μm/minute). Those values decreased in a nearly parallel manner, demonstrating that fl-F-actin flows rearward, towards the posterior end of the cell.

frames (Fig. 4A). The cell's geometric profile and its center ('centroid') were determined from the phase-contrast image (Fig. 4C). The result shows that the centroid moves at an average velocity of 2.14 μm/minute (Fig. 4D). Note that the transient decrease in the velocity (arrow) coincides with the change of the migration direction (Fig. 4A: frames c-d) and the sudden decrease (double headed arrow) was apparently caused by the contact inhibition as indicated by the whole sequence

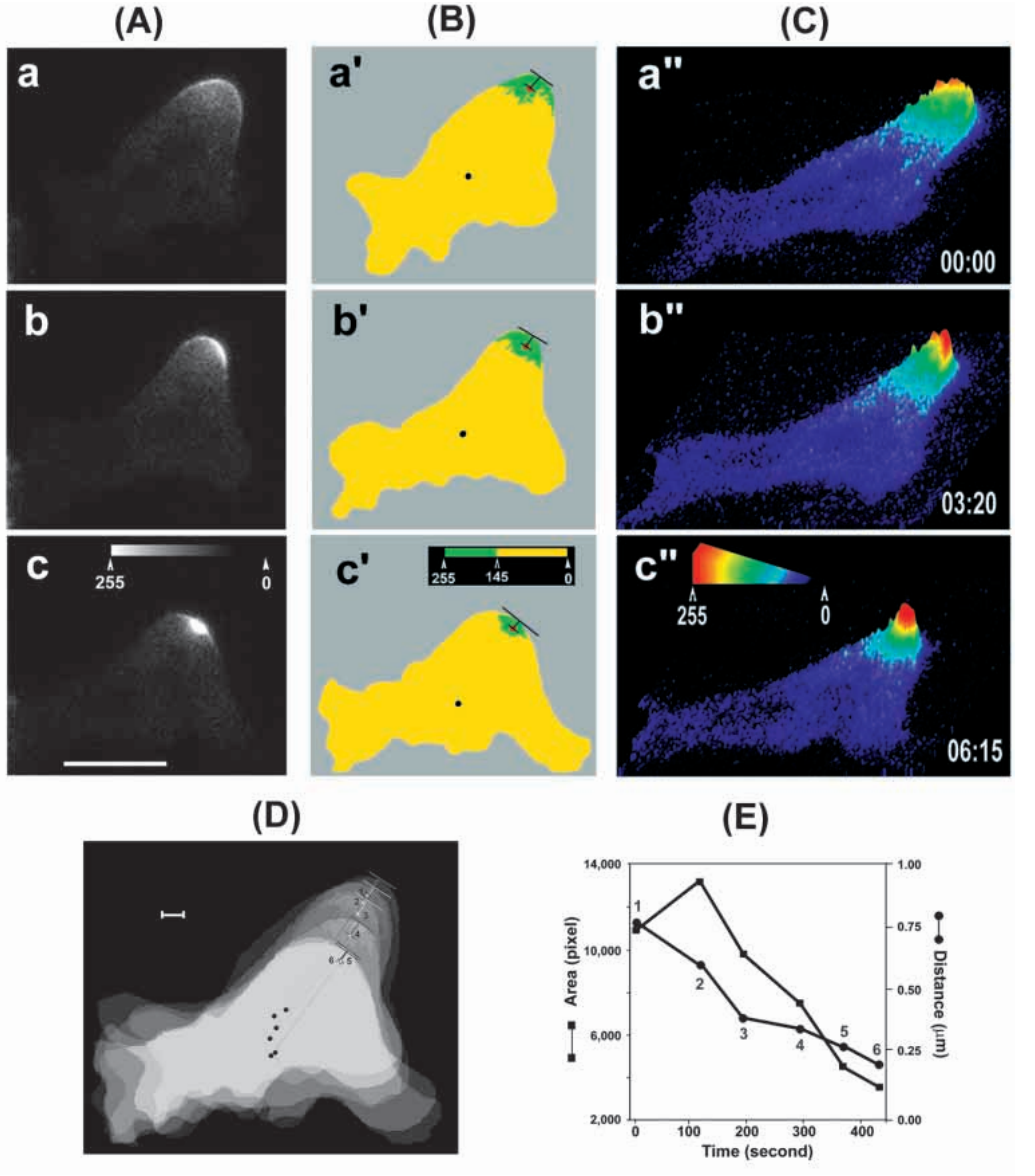

Fig. 5. Representative sequence demonstrating the retrograde flow of F-actin in myosin II null (*mhcA*⁻) amoebae. (For the complete sequence, see the movie at our Web site). (A) Fluorescence sequence. (B) Fluorescence morphometry, showing the shape change (yellow), geometric center (centroid: black dot), the high intensity area (green) and the intensity center (red dot). (C) 3-D intensity profile, illustrating the accumulation of fl-F-actin into the posterior cortex. The intensity of each point (X, Y) was translated into a line (Z) whose length and the color represent its intensity. Time in min:sec. Bar, 5 μm. (D) The diagram illustrating the integrated mode of the cell behavior made from B. The distance between the intensity center and the posterior end are sequentially numbered where 1, 3, and 5 correspond to frames a, b, and c in A. Black dot = centroid. The average centroid movement = 0.38 μm/minute. Bar, 1 μm. (E) The accumulation of the high intensity area (green area; B), and the movement of the intensity center (red dot; panel-B) towards the posterior end. The intensity center moved at an average velocity of 0.07 μm/minute. The data demonstrate that the retrograde flow of F-actin does not require myosin II.

(see movie). The intensity measurements of the high intensity area (Fig. 4B: green area) quantitatively demonstrated that both the area of high intensity and the distance between the intensity center and the tail end of the cell linearly decreases at an average velocity of 0.35 μm/minute (Fig. 4E). These results clearly demonstrate the occurrence of retrograde flow of F-actin towards the tail of migrating amoebae.

The retrograde flow of F-actin occurs in myosin II null (*mhcA*⁻) cells

Since the observed pattern of F-actin accumulation in the posterior cortex is similar to the published myosin II organization in fixed and live amoebae (Yumura et al., 1984; Chu and Fukui, 1996), we examined if the flow also occurs in myosin II null (*mhcA*⁻) cells. The results demonstrated that the retrograde flow does not absolutely require myosin II. A representative sequence shows selected three frames from a total of 33 frames (Fig. 5A: The complete sequence can be seen at our Web site). The result shows that the high intensity area decreases in size and distance from the tail end (Fig. 5B) in a similar manner to that observed in the wild-type cell (Fig. 4). The three-dimensional profile of the intensity (Fig. 5C) illustrates the mode of accumulation into the posterior cortex, in which the gray scale of each point (X, Y) is exemplified by a color-coded line (Z). The panel clearly demonstrates that there is a gradual flow of fl-F-actin originating from the middle cytoplasm (blue-green) and concentrating into the intensity center located in the posterior cell end (orange-red).

The fluorescence morphometric analysis further shows that the centroid moved at an average velocity of 0.38 μm/minute (Fig. 5D), more than 5 times slower than the wild type. The area of high intensity and the distance between the intensity center and the tail end also decreased almost linearly (Fig. 5E), and the velocity of the intensity center movement was 0.07 μm/minute, which was also 5 times slower than the wild type. The slow rate of the F-actin flow is thought to be related to the slow rate of migration of these mutant cells but the exact reason is yet to be determined.

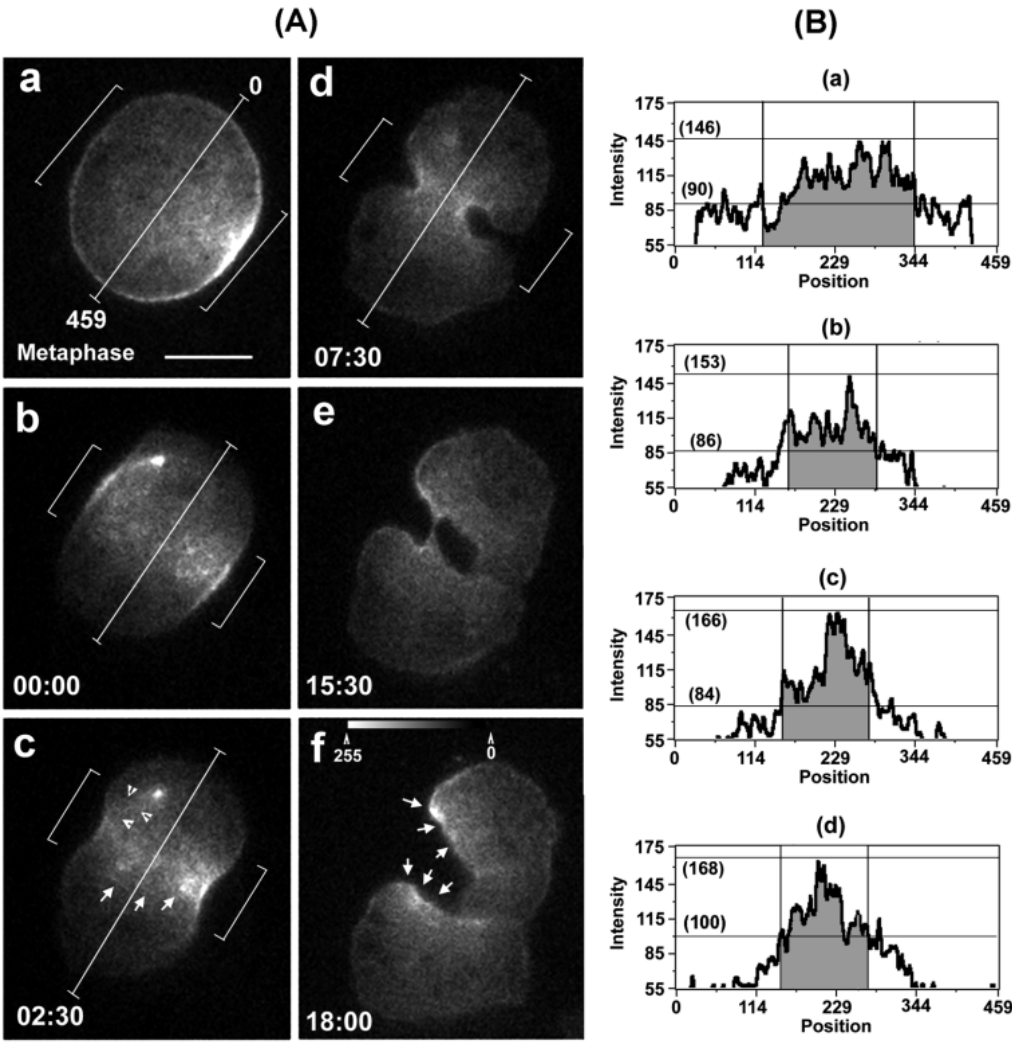

Fig. 6. F-actin flow towards the cleavage furrow. (A) A representative fluorescence sequence demonstrating the movement of fl-F-actin. The intensity was measured along a 10-pixel-wide line labeled with 0/459. The brackets show the approximate width of the cleavage furrow. Note that some F-actin fibrils appear in parallel (c: arrows) or random orientation (c: arrowheads). Arrows (f): cortical accumulation after separation into daughter cells. Time in min:sec. Bar, 5 μm. (B) The intensity profile of the first 4 panels in A. (a) Metaphase, (b) telophase, (c,d) early and middle cytokinesis. The increase in peak intensity at the furrow (shaded area) relative to the ground cytoplasm (horizontal lines) are 60% (a), 80% (b), 100% (c), and 70% (d). The actual image was acquired every 75 seconds, and the whole sequence can be seen at our Web site.

F-actin accumulates into the cleavage furrow during cytokinesis

To assess a role of the observed F-actin flow in the generation of traction forces, we examined the amoebae undergoing cytokinesis. The results show that cortical F-actin slowly accumulates into the cleavage furrow as shown in a representative sequence (Fig. 6A: six selected frames from sixteen that can be seen at our Web site). Some frames indicate the presence of 2-2.5 μm-long fibrous F-actin in the cleavage furrow (Fig. 6A-c), either oriented perpendicular to the pole-to-pole axis (c: arrows) or randomly oriented (c: arrowheads). At the end of cytokinesis, F-actin was re-assembled into the cortex (e-f) and integrated into the posterior domain of the daughter cells (f: arrows).

The intensity measurement clearly demonstrates that F-actin progressively concentrated into the cleavage furrow (Fig. 6B). The increase in the peak intensity, relative to the basal cytoplasm was 60% (a: metaphase), 80% (b: telophase), 100% (c: early cytokinesis), and 70% (d: mid-cytokinesis). This increase is significantly higher than the accumulation of the total actin as demonstrated by our recent study (ca. 20%: Yumura and Fukui, 1998), indicating that a considerable accumulation of F-actin at the cleavage furrow results from lateral transport of cortical F-actin. We do believe, however, that the absolute constriction of the furrow requires the establishment of the contractile ring (Schroeder, 1968), which is responsible for generating the actomyosin II-based contractile forces.

DISCUSSION

Fl-F-actin manifests defined dynamics of cortical F-actin

When injected into live cells, phalloidin and its fluorescent derivatives have been shown to preferentially bind preexisting F-actin and only secondarily bind nascent F-actin causing aberrant filaments and induce decreased locomotion and growth (Wehland et al., 1980). By controlled injections, the fluorescent phalloidin has been successfully used for studying the F-actin dynamics in various cell types (Wehland and Weber, 1981; Hamaguchi and Mabuchi, 1982; Cao and Wang, 1990; Schmit and Lambert, 1987; Lee et al., 1997; Terasaki, 1996). In this study, we observed that microinjected fl-phalloidin does not incorporate into the pseudopods. F-actin of *Dictyostelium* pseudopodia has been shown to be organized into a 3-D network (Cox et al., 1995) and known to be more rapidly exchanging (Condeelis, 1993). It seems very likely that

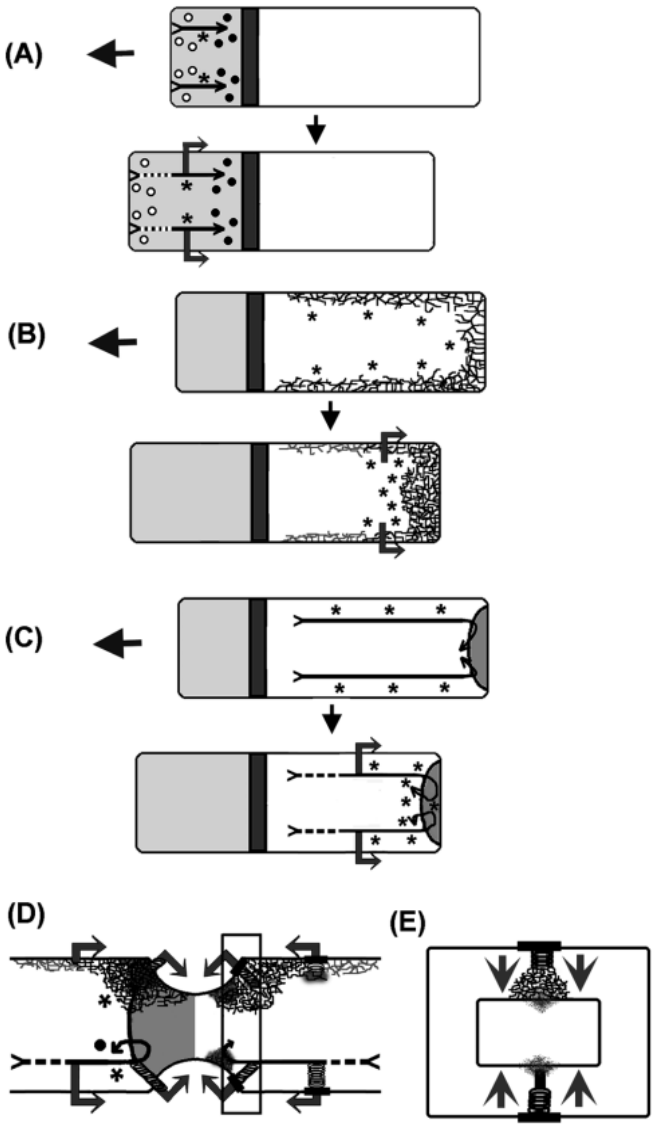

Fig. 7. Diagrams illustrating possible models and their feasibility for the observed F-actin flow in *Dictyostelium*. (A) A simplified diagram illustrating the general retrograde flow model proposed for the lamellipodia or filopodia projection in higher organisms. Note that this diagram is presented only for comparison, and the 'cortical expansion' model represents the possible mechanism for the pseudopodial protrusion in *Dictyostelium* (Condeelis, 1993). (B) The first model suggesting the rearward flow of short, randomly oriented F-actin bound to the membrane. This model presumes the organization of cortical F-actin into meshworks surrounding the posterior cell body, and the *gelation* in the posterior end pulls the entire meshwork towards the rear. If F-actin is linked to the surface, this flow should be translated into traction forces (arrows). (C) The second model presuming the organization of cortical F-actin into bundles. This model is consistent with the observed F-actin flow and reported transport of ConA beads (Jay and Elson, 1992). This model assumes that F-actin interacts with the posterior cortex with some factor(s) and loops back into the cytoplasm where they disassemble into G-actin (left). (D) A diagram suggesting that the above models are also responsible for the cleavage furrow formation. The flow of F-actin will generate cortical tension (arrows) that can constrict the furrow. (E) An imaginary cross section view of the area marked with box in D. The diagram suggests that the movement of F-actin produces the cortical tension which tugs on the plasma membrane like a purse string (arrows). Note that all these models account for the actin-based traction forces only.

fl-phalloidin does not assemble into this class of F-actin in *Dictyostelium*.

In contrast, fl-phalloidin was incorporated into the cortical actin layer. We demonstrated that the fl-F-actin exhibits a cyclic tightening and loosening mode of dynamic. We rationalized that, in two-dimensional cells prepared by the agar-overlay method: (1) the intensity change, in principle, reflects the concentration dynamics; and (2) the positional change relative to the substratum can be interpreted in the same way as the particle movement. The cells exhibiting the fl-F-actin dynamics performed an apparently normal cytokinesis, and eventually, the fl-F-actin dissipated after many hours of observation. These observations lead us to believe that the fl-F-actin dynamics examined in this study correctly reported the bona fide architectural dynamics of the cortical F-actin.

The observed F-actin flow indicates a myosin II-independent force generation mechanism

Previously, in *Dictyostelium*, Jay and Elson (1992) analyzed the mode of transport of ConA-beads in wild-type and myosin II null cells. They found that a similar mode of transport occurs in the myosin II null cells (at a slower speed). The F-actin flow observed in the present study is thought to contribute to both cell locomotion and the particle transport. In fact, we showed that F-actin flows rearward only when the cells migrate forward (Figs 3, 4). In myosin II null cells, we found that F-actin also moves rearward but at a rate much slower than the wild type. We also found that the rate of F-actin flow is 5 times slower than the rate of cell migration in both wild type and the mutant (Fig. 4). The evidence above collectively indicates that at least a part of the observed F-actin flow occurring in the posterior cell body is myosin II-independent. The apparent correlation of the rate of F-actin flow to the rate of cell migration further suggests that this F-actin flow is responsible for the impaired but still competent migration of the myosin II null cells.

Is our observation consistent with the conventional cortical flow model?

The 'cortical flow' of surface materials and certain cellular structures is generally thought to be the phenomenon depicting a long-range, net retrograde flux of actin by virtue of the treadmilling mechanism (Bray and White, 1988; Forscher and Smith, 1988; Fisher et al., 1988; Cao and Wang, 1990). In fibroblasts, however, Symons and Mitchison (1991) showed that F-actin in the lamellipodium disassembles throughout its length, resulting in a gradient of filament density in the lamella. More conflicting evidence was obtained by Theriot and Mitchison (1991, 1992), who challenged the general cortical flow model by examining the F-actin dynamics in fish keratocyte. They showed that, in the lamella, relatively short and randomly oriented actin filaments move rearward after being released from the leading edge. It seems that the exact mechanistics of the actin dynamics and its role in locomotion in the higher organisms are still under controversy (Heath and Holifield, 1991a; Cramer et al., 1994; Small, 1994).

Note that the retrograde flow of F-actin demonstrated in the present study is distinct from known F-actin flow in other

systems. First, the flow occurs in the cortex of the *posterior* cell body but not in the leading edges. Second, the F-actin manifesting the flow is composed of the cortical actin layer encompassing the entire cell body *behind* the pseudopodium. Third, the axial length on the cell body that manifests the flow shortens when the cell migrates. This is in marked contrast to the lamellipodia or filopodia that protrude with respect to the base of the structures. More importantly, the observed direction of the flow (i.e. retrograde) is hardly rationalized based on the generally believed mode of attachment of F-actin to the membranes (see below for details).

Suggested mechanism

An a priori condition for the existing treadmilling models is the barbed end binding of F-actin at the leading edge, and the force transduction by virtue of cross linkage between F-actin and the substrate which can push the *anterior* cell body forward (Fig. 7A). In *Dictyostelium*, F-actin organizes into 3-D meshworks in the pseudopodium, and the mechanism for its protrusion has been suggested to be distinct from that of lamellipodia or filopodia in higher organisms (‘cortical expansion’ model; Condeelis, 1993).

The observed retrograde flow of F-actin *in the posterior cell body* best fits the models illustrated in Fig. 7B and C. In these models, the cortical F-actin is transported rearward either by condensation of the meshwork (model-B) or treadmilling of the filament bundles (model-C). These models also assume that the posterior cortex consists of a unique motif in the components and structure. The first model (B) presumes that the cortical F-actin is organized into the meshwork made of short filaments and they are interconnected by actin-binding proteins. The traction forces are thought to result either from the gelation (condensation into three-dimensional, high-density network) or by virtue of the activity of unconventional myosin(s).

The second model (C) assumes that the cortical F-actin is organized into bundles, and each filament is pointing towards the posterior end. The addition of G-actin predominantly to the barbed end results in the rearward flow. Since it is unlikely that F-actin binds the posterior membrane (or its vicinity) with its pointed end, we presume that F-actin may interact with the posterior end through unknown factors. Given this orientation, the overall direction of the flow of F-actin must be retrograde (Fig. 7C). Although the forces that carry F-actin rearward do not absolutely require myosin II, possible participation of unconventional myosin(s) is worth to be explored.

We suggest that the F-actin flow towards the cleavage furrow can be accounted for by the same mechanism. The longitudinal (Fig. 7D) and the cross sectioned (Fig. 7E) views illustrate this possibility. In Fig. 7D, the right half of the diagram suggests the occurrence of two modes of association of F-actin to the plasma membrane; i.e. (1) cross links with postulated membrane proteins (black cuboid) and (2) lateral association at the pointed end (amorphous shade). In D and E, the two possible models are incorporated into the top and bottom halves. In the cross section view of the highlighted area (Fig. 7E), the arrows indicate the direction of hypothetical forces driven by the flow of F-actin towards the cleavage furrow. These actin-based forces may be responsible for the initial constriction of the furrow.

In conclusion, the present study demonstrated that F-actin flows rearward in the posterior cell body of migrating *Dictyostelium* amoebae and at least a part of this flow is independent of myosin II. We suggest that this flow is responsible for the generation of traction forces for cell migration and furrowing. Importantly, the existing cortical flow and actin treadmilling models alone are hardly applicable to rationalize this movement.

We thank Dr James Spudich’s laboratory of Stanford University School of Medicine for the gift of the *mhcA*$^{-}$ mutant. We thank Dr Edward Kuczmarski for his valuable comments on the manuscript. We thank Robert Valadka and Maya Moody for their help in computing and digital printing. T.K.-Y. was a postdoctoral fellow, and S.Y. was on sabbatical leave from Yamaguchi University. Supported by NIH RO1 GM39548 to Y. F.

REFERENCES

Abercrombie, M., Heaysman, J. E. and Pegrum, S. M. (1970). The locomotion of fibroblasts in culture. III. Movements of particles on the dorsal surface of the leading lamella. *Exp. Cell Res*. **62**, 389-398.

Alberts, B., Bray, D., Lewis J., Raff, M., Roberts, K. and Watson, J. D. (1994). *Molecular Biology of the Cell*, 3rd edn. pp. 846. Garland Publishing, Inc., New York.

Bray, D. (1970). Surface movements during the growth of single explanted neurons. *Proc. Nat. Acad. Sci. USA* **65**, 905-910.

Bray, D. and White, J. G. (1988). Cortical flow in animal cells. *Science* **239**, 883-888.

Cao, L.-G. and Wang, Y.-L. (1990). Mechanism of the formation of contractile ring in dividing cultured animal cells. II. Cortical movement of microinjected actin filaments. *J. Cell Biol.* **111**, 1905-1911.

Carlier, M.-F. (1998). Control of actin dynamics. *Curr. Opin. Cell Biol*. **10**, 45-51.

Chu, Q. and Fukui, Y. (1996). In vivo dynamics of myosin II in *Dictyostelium* by fluorescent analogue cytochemistry. *Cell Motil. Cytoskel.* **35**, 254-268.

Condeelis, J. (1993). The formation of cell protrusions. *Annu. Rev. Cell Biol.* **9**, 441-444.

Cox, D., Ridsdale, J. A., Condeelis, J. and Hartwig, J. (1995). Genetic deletion of ABP-125 alters the three-dimensional organization of actin filaments in *Dictyostelium* pseudopods. *J. Cell Biol*. **128**, 819-835.

Cramer, L. P., Mitchison, T. J. and Theriot, J. A. (1994). Actin-dependent motile forces and cell motility. *Curr. Opin. Cell Biol*. **6**, 82-86.

Cramer, L. P., Siebert, M., and Mitchison, T. J. (1997). Identification of novel graded polarity actin filament bundles in locomoting heart fibroblasts: Implications for the generation of motile force. *J. Cell Biol*. **136**, 1287-1305.

Dembo, M. and Harris, A. K. (1981). Motion of particles adhering to the leading lamella of crawling cells. *J. Cell Biol*. **91**, 528-536.

Fisher, G. W., Conrad, P. A., DeBiasio, R. L. and Taylor, D. L. (1988). Centripetal transport of cytoplasm, actin, and the cell surface in lamellipodia of fibroblasts. *Cell Motil. Cytoskel*. **11**, 235-247.

Forscher, P. and Smith, S. J. (1988). Actions of cytochalasins on the organization of actin filaments and microtubules in a neuronal growth cone. *J. Cell Biol*. **107**, 1505-1516.

Fukui, Y. and Yumura, S. (1986). Actomyosin dynamics in chemotactic amoeboid movement of *Dictyostelium*. *Cell Motil. Cytoskel*. **6**, 662-673.

Fukui, Y. and Inoué, S. (1991). Cell division in *Dictyostelium* with special emphasis on actomyosin organization in cytokinesis. *Cell Motil. Cytoskel.* **18**, 41-54.

Fukui, Y. (1993). Toward a new concept of cell motility: Cytoskeletal dynamics in amoeboid movement and cell division. *Int. Rev. Cyt*. **144**, 85-127.

Fukui, Y. and Inoué, S. (1997). Amoeboid movement anchored by eupodia, new actin-rich knobby feet in *Dictyostelium. Cell Motil. Cytoskel*. **36**, 339-354.

Grebecki, A. (1994). Membrane and cytoskeleton flow in motile cells with emphasis on the contribution of free-living amoebae. *Int. Rev. Cyt.* **148**, 37-80.

Hamaguchi, Y. and Mabuchi, I. (1982). Effects of phalloidin microinjection and localization of fluorescein-labeled phalloidin in living sand dollar eggs. *Cell Motil*. **2**, 103-113.

Harris, A. K. (1973). Cell surface movements related to cell locomotion. In *Locomotion of Tissue Cells* (ed. R. Porter and D. W. FitzSimons), pp. 3-26. Associated Scientific Publishers, Amsterdam.

Harris, A. K. (1994). Locomotion of tissue culture cells considered in relation to ameboid locomotion. *Int. Rev. Cytol*. **150**, 35-68.

Heath, J. and Holified, B. (1991a). Actin alone in lamellipodia. *Nature* **352**, 107-108.

Heath, J. P. and Holifield, B. F. (1991b). Cell locomotion: new research tests old ideas on membrane and cytoskeletal flow. *Cell Motil. Cytoskel*. **18**, 245-257.

Holifield, B. F., Ishihara, A. and Jacobson, K. (1990). Comparative behavior of membrane protein-antibody complexes on motile fibroblasts: Implications for a mechanism of capping. *J. Cell Biol*. **111**, 2499-2512.

Jacobson, K., O'Dell, D., Holifield, B., Murphy, T. L. and August, J. T. (1984). Redistribution of a major surface glycoprotein during cell movement. *J. Cell Biol*. **99**, 1613-1623.

Jay, P. Y. and Elson, E. L. (1992). Surface particle transport mechanism independent of myosin II in *Dictyostelium*. *Nature* **356**, 438-440.

Lee, E., Shelden, E. A. and Knecht, D. A. (1997). Changes in actin filament organization during pseudopod formation. *Exp. Cell Res*. **235**, 295-299.

Lee, J., Gustafsson, M., Magnusson, K.-E. and Jacobson, K. (1990). The direction of membrane lipid flow in locomoting polymorphonuclear leukocytes. *Science* **247**, 1229-1233.

Lee, J., Ishihara, A., Theriot, J. A. and Jacobson, K. (1993). Principles of locomotion for simple-shaped cells. *Nature* **362**, 167-171.

Lin, C. H., Espreafico, E. M., Mooseker, M. S. and P. Forscher (1996). Myosin drives retrograde F-actin flow in neuronal growth cones. *Neurons* **16**, 769-782.

Manstein, D. J., Titus, M. A., De Lozanne, A. and Spudich, J. A. (1989). Gene replacement in *Dictyostelium*: Generation of myosin null mutants. *EMBO J*. **8**, 923-932.

Pollard, T. D. and Craig, S. W. (1982). Mechanism of actin polymerization. *Trends Biochem. Sci*. **7**, 55-58.

Schmit, A. C. and Lambert, A. M. (1987). Characterization and dynamics of cytoplasmic F-actin in higher plant endosperm cells during interphase, mitosis, and cytokinesis. *J. Cell Biol.* **105**, 2157-2166.

Schroeder, T. E. (1968). Cytokinesis: Filaments in the cleavage furrow. *Exp. Cell Res*. **53**, 272-318.

Shaffer, B. M. (1962). The Acrasina. In *Advances in Morphogenesis*, vol. 2 (ed. M. Abercrombie and J. Brachet), pp. 109-182. Academic Press, New York.

Sheetz, M. P., Turney, S., Qian, H. and Elson, E. L. (1989). Nanometre-level analysis demonstrates that lipid flow does not drive membrane glycoprotein movements. *Nature* **340**, 284-288.

Small, J. V. (1981). Organization of actin in the leading edge of cultured cells: Influence of osmium tetroxide and dehydration on the ultrastructure of actin meshworks. *J. Cell Biol*. **91**, 695-705.

Small, J. V. (1994). Lamellipodia architecture: actin filament turnover and the lateral flow of actin filaments during motility. *Semin. Cell Biol.* **5**, 157-163.

Small, J. V., Isenberg, G. and Celis, J. E. (1978). Polarity of actin at the leading edge of cultured cells. *Nature* **272**, 638-639.

Svitkina, T. M., Neyfakh, Jr, A. A. and Bershadsky, A. D. (1986). Actin cytoskeleton of spread fibroblasts appears to assemble at the cell edges. *J. Cell Sci*. **82**, 235-248.

Symons, M. H. and Mitchison, T. J. (1991). Control of actin polymerization in live and permeabilized fibroblasts. *J. Cell Biol*. **114**, 503-513.

Terasaki, M. (1996). Actin filament translocations in sea urchin eggs. *Cell Motil. Cytoskel*. **34**, 48-56.

Theiot, J. A. and Mitchison, **T. J.** (1991). Actin microfilament dynamics in locomoting cells. *Nature* **352**, 126-131.

Theriot, J. A. and Mitchison, T. J. (1992). The nucleation-release model of actin filament dynamics in cell motility. *Trends Cell Biol*. **2**, 219-221.

Tilney, L. G. and Inoué, S. (1985). Acrosomal reaction of *Thyone* sperm. III. The relationship between actin assembly and water influx during the extension of the acrosomal process. *J. Cell Biol*. **100**, 1273-1283.

Wang, Y.-L. (1985). Exchange of actin subunits at the leading edge of living fibroblasts: Possible role of treadmilling. *J. Cell Biol*. **101**, 597-602.

Wang, Y.-L. (1987). Mobility of filamentous actin in living cytoplasm. *J. Cell Biol*. **105**, 2811-2816.

Wehland, J., Osborn, M. and Weber, K. (1980). Phalloidin associates with microfilaments after microinjection into tissue culture cells. *Eur. J. Cell Biol*. **21**, 188-194.

Wehland, J. and Weber, K. (1981). Actin rearrangement in living cells revealed by microinjection of a fluorescent phalloidin derivative. *Eur. J. Cell Biol*. **24**, 176-183.

Yumura, S., Mori, H. and Fukui, Y. (1984). Localization of actin and myosin for the study of amoeboid movement in *Dictyostelium discoideum* using improved immunofluorescence. *J. Cell Biol*. 99, 894-899.

Yumura, S. and Kitanishi-Yumura, T. (1990). Fluorescence-mediated visualization of actin and myosin filaments in the contractile membrane-cytoskeleton complex of *Dictyostelium discoideum*. *Cell Struct. Funct*. **15**, 355-364.

Yumura, S. (1996). Spatial distribution of fluorescently labeled actin in living *Dictyostelium* amoebae. *Cell Struc. Funct.* **21**, 189-197.

Yumura, S. and Fukui, Y. (1998). Spatiotemporal dynamics of actin concentration during cytokinesis and locomotion in *Dictyostelium*. *J. Cell Sci*. **111**, 2097-2108.